ChemComm

COMMUNICATION

View Article Online
View Journal | View Issue

Cite this: *Chem. Commun.*, 2016, 52, 13144

Received 6th July 2016,
Accepted 13th October 2016

DOI: 10.1039/c6cc05599k

www.rsc.org/chemcomm

Green-to-red primed conversion of Dendra2 using blue and red lasers†

N. V. Klementieva,[a] K. A. Lukyanov,[ab] N. M. Markina,[b] S. A. Lukyanov,[abc] E. V. Zagaynova[a] and A. S. Mishin*[ab]

Recently, an unusual phenomenon of primed conversion of fluorescent protein Dendra2 by combined action of blue (488 nm) and near-infrared (700–780 nm) lasers was discovered. Here we demonstrate that primed conversion can be induced by red lasers (630–650 nm) common for most confocal and single molecule detection microscopes.

Photoactivatable fluorescent proteins (PAFPs) capable of strong light-induced increase of fluorescence intensity at certain wavelengths can be used for direct tracking of the movement of target proteins, cell organelles or cells in live models.[1] Even more importantly, PAFPs represent genetically encoded labels of choice for super-resolution fluorescence microscopy.[2–4]

There are many types of PAFPs possessing either reversible or irreversible photoconversion in response to light illumination at different wavelengths. Among them, green-to-red photoconvertible proteins are especially popular. The first member of this protein group named Kaede was identified in a stony coral.[5] Kaede is a tetrameric protein that matures up to a green fluorescent state in the dark. Then, it can be efficiently converted into a red fluorescent state by illumination with UV-violet light (approximately 350–410 nm). Monomeric variants of some Kaede-like proteins suitable for protein labeling were engineered. In particular, monomeric Dendra and its improved version Dendra2 were generated from a tetrameric wild type protein from an octocoral *Dendronephthya*.[6] It has been demonstrated that Dendra2 is a useful tool to follow cell[7] and protein movement[6,8,9] and turnover[10,11] as well as for subdiffraction localization microscopy.[12,13]

Dendra(2) was found to be convertible not only by UV-violet (*e.g.*, 405 nm) but also by blue (*e.g.*, 488 nm) light.[6,8] However, the photoconversion by blue light is 25-fold less efficient.[14]

Recently, an unusual phenomenon of two-stage primed photoconversion was discovered in Dendra2 and mEos2. Specifically, a near-infrared light applied with the 'priming' blue light simultaneously or in rapid succession increases the efficiency of the photoconversion by an order of magnitude compared to action of the blue light alone.[15] Wavelengths from 700 to 1000 nm were tested; a 700–780 nm spectral region was found to be optimal. The suggested dual-laser (488 + 730 nm at a roughly 1 : 100 intensity ratio) illumination scheme avoids the need for short-wavelength violet (405 nm) light, which was shown to induce various phototoxic effects in live cell microscopy.[16] Also, it enables controlled photoconversion in a spatially confined intersection of the two laser beams.[15,17]

At the same time, many fluorescence microscopes come with a red laser source, with a wavelength almost 100 nm shorter than reported to be necessary for the primed photoconversion. Here, we tested the effect of combined illumination using blue and red light sources on Dendra2 photoconversion.

First, we performed green-to-red photoconversion of purified Dendra2 protein solution in a cuvette using light emitting diodes (LEDs). We observed clearly detectable photoconversion by combination of blue (470 nm) and red (655 nm) LEDs, whereas separate illumination with these LEDs resulted in much weaker (blue LED) or no detectable (red LED) photoconversion (Fig. S1a, ESI†). Excitation and emission spectra of the Dendra2 red form obtained by primed conversion (470 + 655 nm) were indistinguishable from that resulting from 400 nm LED-induced conversion (Fig. S1b, ESI†). A similar coincidence of the spectra was observed for near-infrared-induced primed conversion.[15]

Next, we tested Dendra2 primed conversion using a regular laser scanning confocal microscope. Beads with immobilized Dendra2 were scanned with a 488 nm laser of varied intensities (8–190 kW cm^{-2}) either alone or in combination with 100% power of the 633 nm laser (450 kW cm^{-2}, ESI†). A strong increase of photoconversion efficiency by co-illumination with the 633 nm laser was observed for all tested intensities of the 488 nm line, whereas the 633 nm laser alone induced no detectable photoconversion (Fig. 1).

[a] *Nizhny Novgorod State Medical Academy, Nizhny Novgorod, Russia*
[b] *Shemyakin-Ovchinnikov Institute of Bioorganic Chemistry, Moscow, Russia. E-mail: mishin@ibch.ru*
[c] *Pirogov Russian National Research Medical University, Moscow, Russia*

† Electronic supplementary information (ESI) available: Supplementary figures and methods. See DOI: 10.1039/c6cc05599k

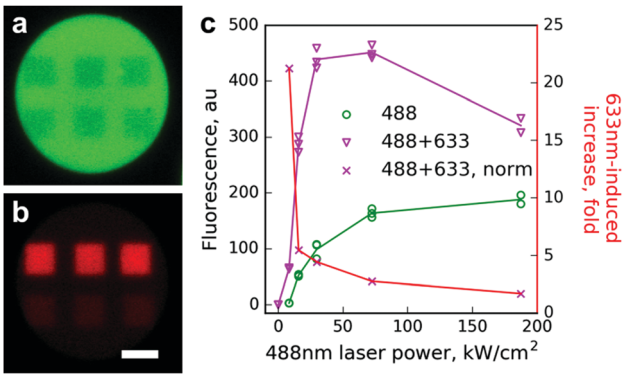

Fig. 1 Photoconversion of Dendra2 immobilized on beads using a laser scanning confocal microscope. (a and b) Images of a bead in green (a) and red (b) channels after Dendra2 photoconversion within six small rectangular regions using either simultaneous scanning with 488 and 633 nm lasers (upper regions) or a 488 nm laser alone (lower regions). Scale bar 10 μm. Note an equal decrease of the green signal but a much stronger increase of the red signal in the case of 488 + 633 nm illumination. (c) Red signal appearance (left ordinate) resulting from conventional (488 nm, green circles) or primed (488 nm + 450 kW cm^{-2} 633 nm, magenta triangles) photoconversion, and the ratio of these red signals at each point (red crosses, right ordinate). In panel (c) individual data points are shown, while the lines are drawn for the mean values.

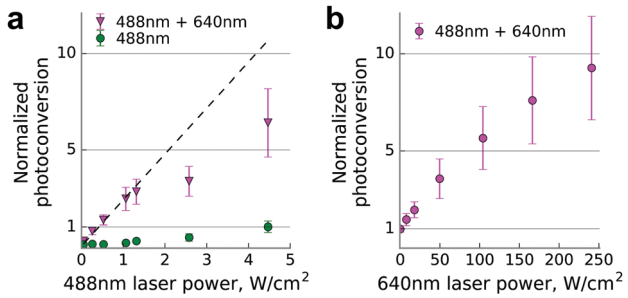

Fig. 2 Dendra2-actin photoconversion in live HeLa Kyoto cells in a wide field regime. (a) Photoconversion efficiency scaling at constant power of the 640 nm laser (240 W cm^{-2}), normalized to the one achievable at the maximum power of the 488 nm laser (4.5 W cm^{-2}). The dashed line shows a linear regression of the first three data points. For any given power (488 nm) value, data points differ significantly from the corresponding 488 nm + 640 nm ones (two-tailed unequal variance *t*-test, $P < 0.001$). (b) Photoconversion efficiency scaling at constant power of the 488 nm laser, set to the value just below the saturation point (1 W cm^{-2}), normalized to the data point without 640 nm illumination. Data are mean ± s.d. (error bars) for $n = 23$ cells.

The effect of primed conversion was especially pronounced (up to 20-fold) at low intensities of the 488 nm laser. Starting from 50 kW cm^{-2} of the 488 nm laser, absolute values of the red signal did not increase and they even decreased. We attributed this to two processes. First, the power of the red laser in our setup might not be sufficient to maintain the high yield of the photoconversion at the given power of the blue laser. Second, strong 488 nm light partially bleaches the newly appearing red form of Dendra2, which possesses considerable absorption at this wavelength in both anionic and neutral states.[14] Indeed, the time course of red signal changes upon illumination using the 488 nm laser of different intensities clearly showed a strong bleaching of the red form by 488 nm light (Fig. S2, ESI†).

Finally, we used a commercial single molecule detection microscope for conversion of Dendra2 fused to β-actin in living cells (Fig. 2). We determined the photoconversion efficiency by illuminating the sample simultaneously with unfocused beams of 640 nm and 488 nm laser lines operating at various power levels, 2–3 orders of magnitude lower than in the confocal setup.

We observed up to 10-fold enhancement in the photoconversion efficiency of Dendra2 in the two-laser illumination scheme. The nonlinear power dependence of the photoconversion strongly resembles the one previously reported for near-infrared illumination.[15]

We then tested the applicability of optimized illumination settings (250 : 1 power ratio of the red and blue lasers, ~1 W cm^{-2} of 488 nm light) for single-molecule localization microscopy. We were able to achieve a similar number of localizations per frame and indistinguishable localization precision in comparison to 405 nm induced photoconversion (Fig. 3). Expectedly, illumination with the 488 nm laser alone

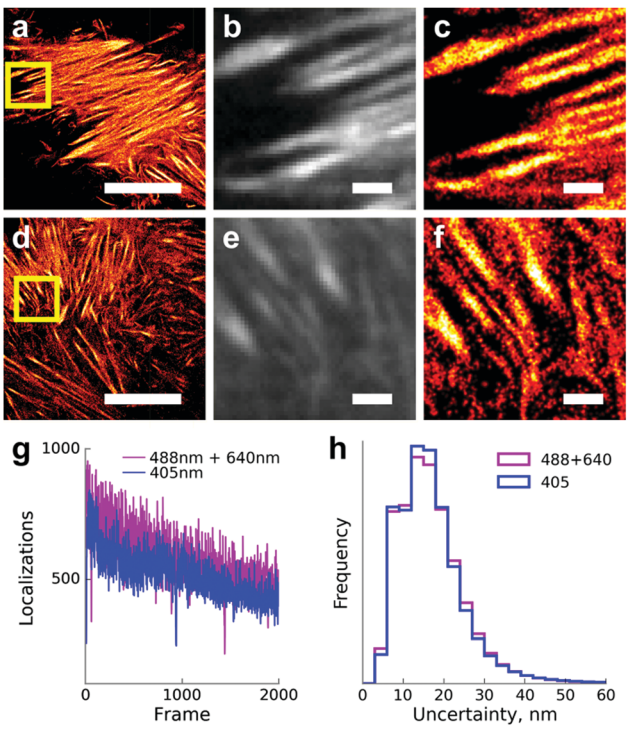

Fig. 3 Single-molecule localization microscopy of live HeLa Kyoto cells expressing Dendra2-Lifeact. (a–c) Primed photoconversion using 488 and 640 nm lasers. (d–f) Conventional photoconversion by the 405 nm laser. (a and d) Super-resolved images, scale bars 10 μm. (b and e) Diffraction-limited images of regions from panels a and d designated by yellow squares. Scale bars 1 μm. (c and f) Super-resolved images of the same regions. Scale bars 1 μm. (g) Number of single-molecule localizations per frame in a time series with conventional and primed photoconversion under the total internal reflection fluorescence (TIRF) illumination mode. (h) Normalized histograms of the localization uncertainties with primed and conventional photoconversion ($n = 10\,000$ localizations). Median localization uncertainty – 18 nm in both cases.

resulted in a much lower number of localizations, inadequate for live-cell super-resolution imaging (Fig. S3, ESI†).

It is difficult to compare the efficiencies of Dendra2 primed conversion using red and infrared lasers because of strong differences in illumination conditions. Dempsey *et al.* reported up to 20-fold increased efficiency of primed conversion relatively to maximal 488 nm-induced conversion (see Fig. 1c and Supplementary Fig. 8 in ref. 15). In our experiments, primed conversion was about 7-fold more efficient compared to maximal conversion achievable by the 488 nm laser alone (see Fig. 2a). Therefore, red lasers appear to be less efficient for primed conversion than infrared ones. However, an accurate comparison would require side-by-side experiments on the same setup in a wide range of illumination settings due to the possible impact of the photobleaching and other sources of non-linearity on the final estimate.

Importantly, dual-wavelength illumination can be a source of unexpected or even undesirable effects. For example, it was demonstrated that photobleaching of cyan fluorescent protein Cerulean increases under simultaneous illumination with 458 and 561 nm lasers compared to the 458 nm alone.[15] Thus, the 458 nm light produces a red-shifted spectral intermediate sensitive to 561 nm illumination. Light-induced appearance of strongly red-shifted long-lived dark states was documented also for other fluorescent proteins of different colors.[3] It urges researchers to take special precautions to avoid artifacts in multicolor imaging with simultaneous or fast sequential illumination of the sample with two or more excitation wavelengths.

In conclusion, we demonstrated that 630–650 nm light can be used to induce primed conversion of Dendra2. The effect was observed in a wide range of illumination intensities, spanning more than three orders of magnitude. As these laser lines are very common in both confocal and super-resolution microscopy, primed conversion requires no additional modifications to commercial setups and hence is broadly available for researchers.

This work was supported by Russian Science Foundation grant 14-25-00129. The work was partially carried out using equipment provided by the IBCH Core Facility (CKP IBCH).

Notes and references

1 K. A. Lukyanov, D. M. Chudakov, S. Lukyanov and V. V. Verkhusha, *Nat. Rev. Mol. Cell Biol.*, 2005, **6**, 885–891.
2 D. M. Shcherbakova, P. Sengupta, J. Lippincott-Schwartz and V. V. Verkhusha, *Annu. Rev. Biophys.*, 2014, **43**, 303–329.
3 A. S. Mishin, V. V. Belousov, K. M. Solntsev and K. A. Lukyanov, *Curr. Opin. Chem. Biol.*, 2015, **27**, 1–9.
4 E. Betzig, G. H. Patterson, R. Sougrat, O. W. Lindwasser, S. Olenych, J. S. Bonifacino, M. W. Davidson, J. Lippincott-Schwartz and H. F. Hess, *Science*, 2006, **313**, 1642–1645.
5 R. Ando, H. Hama, M. Yamamoto-Hino, H. Mizuno and A. Miyawaki, *Proc. Natl. Acad. Sci. U. S. A.*, 2002, **99**, 12651–12656.
6 N. G. Gurskaya, V. V. Verkhusha, A. S. Shcheglov, D. B. Staroverov, T. V. Chepurnykh, A. F. Fradkov, S. Lukyanov and K. A. Lukyanov, *Nat. Biotechnol.*, 2006, **24**, 461–465.
7 W. P. Dempsey, S. E. Fraser and P. Pantazis, *PLoS One*, 2012, **7**, e32888.
8 D. M. Chudakov, S. Lukyanov and K. A. Lukyanov, *Biotechniques*, 2007, **42**, 553, 555, 557 passim.
9 E. Woods, J. Courtney, D. Scholz, W. W. Hall and V. W. Gautier, *J. Microsc.*, 2014, **256**, 197–207.
10 L. Zhang, N. G. Gurskaya, E. M. Merzlyak, D. B. Staroverov, N. N. Mudrik, O. N. Samarkina, L. M. Vinokurov, S. Lukyanov and K. A. Lukyanov, *Biotechniques*, 2007, **42**, 446, 448, 450.
11 P. Müller, K. W. Rogers, B. M. Jordan, J. S. Lee, D. Robson, S. Ramanathan and A. F. Schier, *Science*, 2012, **336**, 721–724.
12 T. J. Gould, M. S. Gunewardene, M. V. Gudheti, V. V. Verkhusha, S.-R. Yin, J. A. Gosse and S. T. Hess, *Nat. Methods*, 2008, **5**, 1027–1030.
13 M. S. Gunewardene, F. V. Subach, T. J. Gould, G. P. Penoncello, M. V. Gudheti, V. V. Verkhusha and S. T. Hess, *Biophys. J.*, 2011, **101**, 1522–1528.
14 N. S. Makarov, C. Cirloganu, J. W. Perry, K. A. Lukyanov and K. M. Solntsev, *J. Photochem. Photobiol., A*, 2014, **280**, 5–13.
15 W. P. Dempsey, L. Georgieva, P. M. Helbling, A. Y. Sonay, T. V. Truong, M. Haffner and P. Pantazis, *Nat. Methods*, 2015, **12**, 645–648.
16 S. Wäldchen, J. Lehmann, T. Klein, S. van de Linde and M. Sauer, *Sci. Rep.*, 2015, **5**, 15348.
17 M. A. Mohr and P. Pantazis, *Methods in Cell Biology*, 2016, pp. 125–138.

